

# International Conference on Space Optics—ICSO 2018

Chania, Greece

9–12 October 2018

*Edited by Zoran Sodnik, Nikos Karafolas, and Bruno Cugny*



## *An absolute frequency reference unit for space borne spectroscopy*

*H. Schaefer*

*D. Heinecke*

*T. Liebherr*

*D. Battles*

*et al.*



icso proceedings



# An absolute frequency reference unit for space borne spectroscopy

H. Schaefer\*<sup>a</sup>, D. Heinecke<sup>a</sup>, T. Liebherr<sup>a</sup>, D. Battles<sup>a</sup>, K. Schleisiek<sup>a</sup>, D. Fehrenbacher<sup>a</sup>, M. Herding<sup>a</sup>, A. Baatzsch<sup>a</sup>, C. Dahl<sup>a</sup>, K. Nicklaus<sup>a</sup>

<sup>a</sup>SpaceTech GmbH, Seelbachstr. 13, D-88090 Immenstaad, Germany

## ABSTRACT

Light detection and ranging (LIDAR) systems have become an important technology in a variety of industrial and scientific applications. In spectroscopy, LIDAR systems can improve the sensitivity by orders of magnitude but require the laser source to have a sufficient small linewidth and stability. For terrestrial applications, such systems have been developed over the last decade and are commercially available. In space, this technology does not have a comparable maturity level and is still far from being a standard technology.

In this paper, we present the design and first measurement results of a spaceborne absolute frequency reference based on the absorption feature at 1645.55 nm of methane gas. The frequency reference unit is used in the instrument of the French-German Methane Remote Sensing LIDAR Mission, MERLIN. It provides the stabilized seed lasers for the high power laser sources at the required wavelengths and measures the absolute frequency of the outgoing laser pulses by means of a wavemeter.

**Keywords:** absolute frequency reference, methane, gas cell, wavemeter, laser diode, absorption spectroscopy, optical reference, InGaAs line detector

## 1. INTRODUCTION

The Frequency Reference Unit (FRU) is part of the light detection and ranging (LIDAR) instrument placed on the satellite of the French-German Methane Remote Sensing LIDAR Mission<sup>1</sup> (MERLIN). For the MERLIN mission absolute frequency accuracy levels in the low MHz range are required in order to be able to detect the atmospheric methane concentration with sufficient resolution.<sup>1</sup> The FRU serves as both, a seeding source with high precision for the optical parametric oscillator (OPO) of the main laser and a high-resolution spectrometer for detection of the generated high power pulses that are sent to earth at the spectroscopic wavelengths around 1645 nm. Additionally, the FRU controls the OPO cavity of the main laser in order to adjust and maintain the cavity length to be resonant to the desired frequency. Moreover, the FRU provides a stable seed source to the master oscillator at the 1064 nm operational wavelength.

In this paper, we present the final design of the FRU.<sup>2</sup> In addition to describing the design, we discuss the critical aspects of the FRU w.r.t. performance, space environment and qualification of the components. The engineering model has been built and is in the final software implementation stage. First performance measurements have been conducted. The most important performance data are summarized at the end of this paper.

\*hanjo.schaefer@spacetechnology.com; phone 49 7545 93284 13; fax 49 7545 93284 60; www.spacetechnology.com

## 2. THE DESIGN OF THE FRU

The FRU consists of free-space optics for the spectroscopic parts, electro-optical components to generate and detect light and a fiber-integrated harness for routing, switching and distributing the light. Analogue and digital electronics including a Field-Programmable Gate Array (FPGA) are used for control and communication purposes and (opto-) mechanical parts for structural and thermal interfacing. The design is described in detail in the next paragraphs.

### 2.1 The functional design of the FRU

The functional and performance requirements of the FRU are:

- Seeding of the 1064 nm master oscillator with an optical power of 10 mW. The seeder wavelength range is  $1064.2 \text{ nm} \pm 0.5 \text{ nm}$  and the required linewidth is smaller than 1 MHz.
- Absolute frequency referencing to the 1645.55 nm (6077  $\text{cm}^{-1}$ ) methane line by stabilizing a laser diode to the local transmission maximum ( $\lambda_{\text{ref}}$ ,  $\lambda_{\text{ref}}$ ) of a low pressure methane gas cell at this wavelength.
- Seeding of the OPO at two wavelengths,  $\lambda_{\text{on}}(\text{seed})$  and  $\lambda_{\text{off}}(\text{seed})$ , referenced to the absolute frequency reference. The nominal frequency offsets relative to  $\lambda_{\text{ref}}$  are -200 MHz for the  $\lambda_{\text{on}}(\text{seed})$  and about -30 GHz for  $\lambda_{\text{off}}(\text{seed})$ . The optical power delivered to the OPO needs to be higher than 5 mW and the linewidth smaller than 2 MHz. The frequency stability of  $\lambda_{\text{on}}(\text{seed})$  needs to be better than 10 MHz and better than 20 MHz for  $\lambda_{\text{off}}(\text{seed})$ .
- Spectroscopic measurement of all individually emitted OPO laser pulses  $\lambda_{\text{on}}(\text{Tx})$  and  $\lambda_{\text{off}}(\text{Tx})$ , relative to  $\lambda_{\text{on}}(\text{seed})$  and  $\lambda_{\text{off}}(\text{seed})$ , where Tx denotes the transmitted pulse.
- Stabilization of the difference between  $\lambda_{\text{on}}(\text{seed})$  and  $\lambda_{\text{on}}(\text{Tx})$ , based on the relative frequency measurement and via a control signal to adjust the OPO cavity length.
- Stabilization of the difference between  $\lambda_{\text{off}}(\text{seed})$  and  $\lambda_{\text{off}}(\text{Tx})$  in order to lock  $\lambda_{\text{off}}(\text{seed})$  to  $\lambda_{\text{off}}(\text{Tx})$ , which is determined by the OPO cavity resonance next to the desired -30 GHz offset.
- Absolute frequency metrology providing a frequency knowledge better than 8 MHz for the online and 50 MHz for the offline frequency for a 7 seconds integration window.

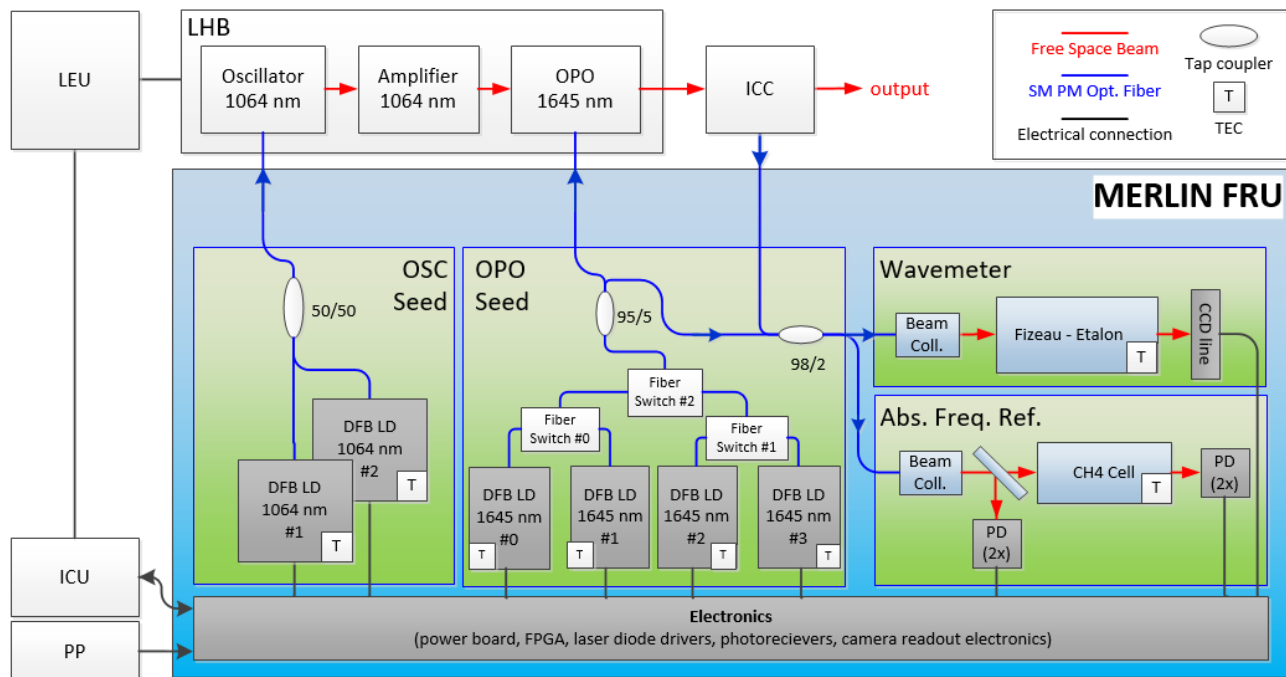


Figure 1. Functional Block Diagram of the FRU

In the next paragraphs, we will explain the different functional blocks of the FRU. An overview over the functional blocks is shown in Figure 1. Apart from the electronics, four main functional blocks are presented: The Maser Oscillator

seeder (OSC-seed), the optical parametric oscillator seeder (OPO-seed), the wavemeter (FRUF) and the absolute frequency reference (FRUA).

## 2.2 Master Oscillator seed

The master oscillator seed (OSC-seed) provides a 10 mW laser light at 1064 nm from a temperature- and current-stabilized laser diode. By temperature tuning, the wavelength can be selected to match the gain maximum of the master oscillator laser. For reliability reasons, two laser diodes are routed to the output port through a combining tap coupler and provide a cold redundancy.

The laser diodes are available from Eagleyard in a space-qualified design flown on GAIA. Due to the larger temperature range on MERLIN, a redesign has been made which increases the stiffness of the modules against thermo-mechanical stress. In addition, optical isolators have been integrated in order to avoid mode-hopping of the lasers upon external back-reflections. To verify these changes and also the different type of chip material that is used for the required wavelength, a screening and a lot acceptance test campaign of the actual FM laser diodes will be performed along the guidelines of ESCC 23201. Environmental testing to MERLIN specifications will be performed. The component will be delivered fully qualified by eagleyard Photonics.

## 2.3 Optical Parametric Oscillator seed

The optical parametric oscillator seed (OPO-seed) provides 5 mW laser light at different wavelengths around 1645.55 nm from temperature- and current-stabilized laser diodes. One out of four laser diodes can be selected and routed to the output through three optical switches. In normal operation, three out of the four laser diodes are active and provide the following functions:

- Seeding the OPO at the online frequency ( $\lambda_{on}$ ),
- Seeding the OPO at the offline frequency ( $\lambda_{off}$ ) and
- Providing the calibration of the wavemeter through the reference frequency ( $\lambda_{ref}$ ).

All laser diodes can provide any of these three functionalities. The fourth laser diode is not active and serves as a cold redundant reserve in case one of the other laser diodes fails to operate properly.

The qualification approach of the laser diodes is the same as for the OSC-seed laser diodes.

## 2.4 The absolute frequency reference (FRUA)

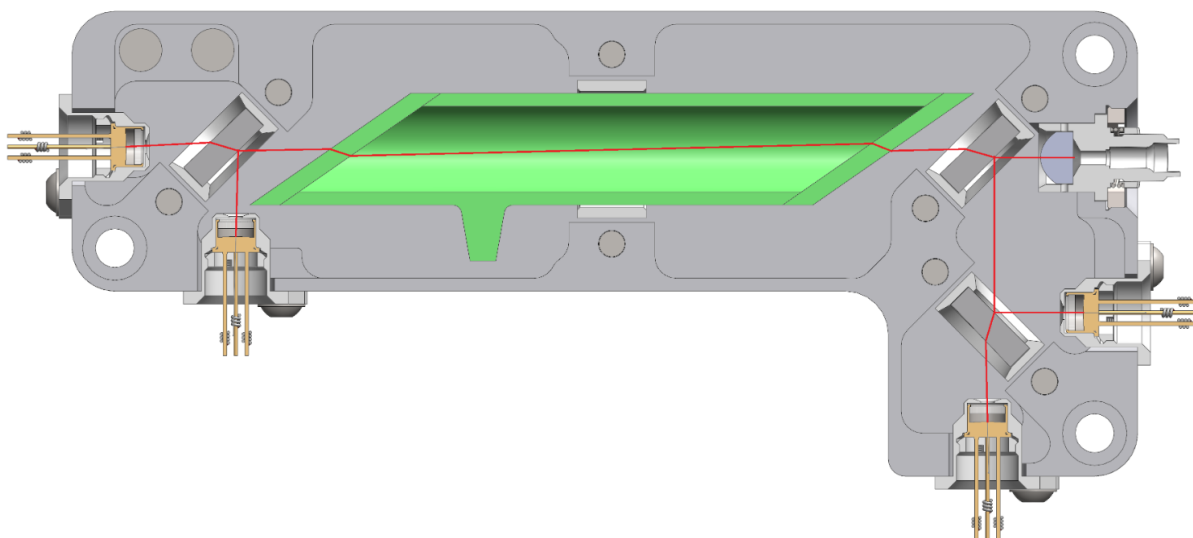


Figure 2. The FRUA assembly: The light (indicated by the red line) launches into the assembly on the upper right side from a fiber connector facing an aspheric lens to collimate the beam. The first beam splitter samples about half of the light power to the reference branch. This again incorporates a beam splitter to steer the light onto two photo diodes for redundant operation. The other part passes through the methane gas cell (shown in green) to be again split onto two photo diodes.

The FRUA provides the absolute frequency calibration of the FRU with respect to the methane gas absorption feature. It ensures that the  $\lambda_{on}$  wavelength maintains its defined value within 10 MHz accuracy and provides the absolute reference to the measured values of  $\lambda_{on}$  and  $\lambda_{off}$ . It consists of a beam collimator, a methane gas cell, three beam splitters and four photodiodes with associated electronics. The assembly is shown in Figure 2. A set of six nearby lines in the methane

spectrum invokes a maximum in transmission in their centre, as shown in , and stems from the same absorption feature that is used by the main laser and instrument to detect the methane concentration in the atmosphere of the Earth.

This feature is scanned with the reference laser diode and used to stabilize the frequency of the reference laser diode by comparing the transmission through the cell on the lower side edge with the upper side edge (red dots in the figure) and levelling them by adjustment of the reference value  $\lambda_{ref}$ , which is indicated by the dashed red line.

The  $\lambda_{ref}$  is measured on the wavemeter where the frequency measurements of all other seeders and the transmit pulses are done and can be evaluated relative to it.

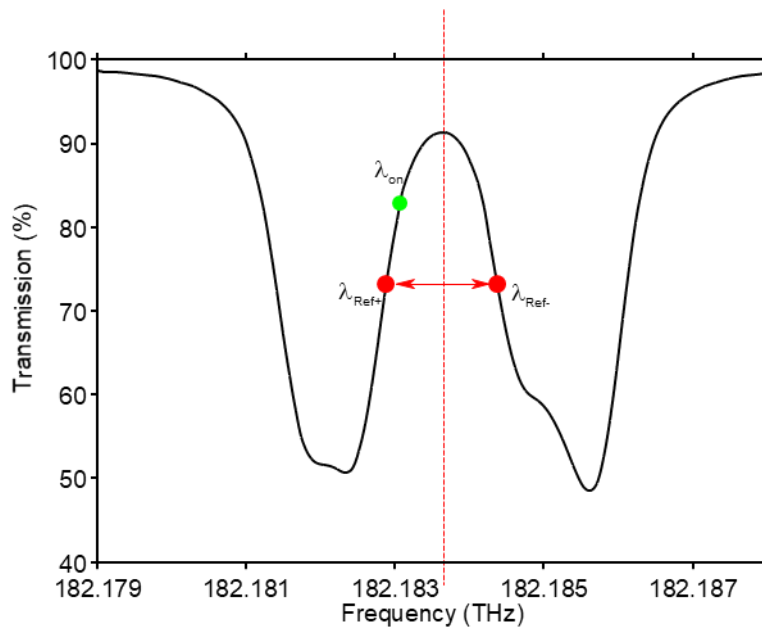


Figure 3. Transmission spectrum through the methane gas cell at 1645.55 nm. The sign of the Ref points (red dots) is defined by the delta currents w.r.t. the  $\lambda_{ref}$  current (center position) that are applied to the laser diode in order to shift its frequency. As higher currents yield higher wavelength but lower frequency, the sign is opposite. The center frequency (dashed red line) is controlled in such a way, that both transmission values have the same level. The green dot indicates roughly the frequency where the OPO is seeded for generating the online pulse.

For the FRUA assembly, a set of InGaAs photo detectors has been procured, which were subjected to a full space qualification. The optical elements will be qualified to the vibrational and shock loads on component or unit level. The coatings are radiation hard by using the  $\text{SiO}_2/\text{Ta}_2\text{O}_5$  material combination. A coating process that ensures dense coatings avoids problems with adsorbed water, which could release under vacuum conditions.

## 2.5 The wavemeter

For frequency measurements of the online and offline seeders, as well as the corresponding OPO transmit pulses, a wavemeter is used. It consists of a monolithic beam collimator, a Fizeau wedge and an InGaAs line detector, as shown in Figure 4.

To generate a well-collimated input beam with a diameter of 12.5 mm, an ultra-high numerical aperture single mode fiber is directly spliced to a single surface aspheric lens. This allows for a very robust collimator design and a short assembly length in order to meet the demanding envelope requirements of the FRU. The Fizeau wedge has a length of 35 mm resulting in free-spectral range of 4.28 GHz. The finesse is about 24. The design does not include a cylindrical lens to focus the fringe pattern on the detector array in order to keep the design simple and to save space. Instead, a slit aperture is used to reduce stray light on the detector. The InGaAs line has 640 pixels with a width of 20 microns.

Figure 5 (bottom) shows an example of the fringe pattern generated by the Fizeau wedge and recorded with the InGaAs line detector. For frequency determination, the position of the centroid of the fringe on the line detector shall be identified. A FPGA-compatible algorithm filters the recorded pattern with a step like filter function as shown in Figure 5. The result represents the low-pass filtered derivative of the fringe. Using a linear regression on this result provides the zero-crossing point with a resolution of 1/16 of a pixel and therefore a measure for the fringe position. The filter function selects only the steep flanks of the upper 75 % of the fringe signal. The algorithm is very robust against amplitude

fluctuations as well as pixel-to-pixel non-uniformities and takes about 142  $\mu$ s to provide the result. Both, the continuous-wave light from the seeders as well as the OPO pulses with a duration of about 20 ns can be measured with the wavemeter. For rather symmetric input spectra, the algorithm coincides with the centroid. In case the OPO spectrum is too asymmetric, offset compensation parameters can be set. The algorithm itself as well as the InGaAs line detector design provide a certain robustness against pixel failures. Two read-out ICs in an odd-even configuration are used for data acquisition and are followed by dedicated 14-bit analogue-digital-converters. The performance of the wavemeter is sufficient with data only from odd or even pixels available; see Figure 6 a). In addition, a bad pixel map is implemented which can be filled by ground-loop actions to mask dark, bright or blinking pixels. Due to the filtering effect of the algorithm, a failure of up to 12 pixels in a row can be tolerated before the performance of the wavemeter drops below the required resolution, compare Figure 6 b).

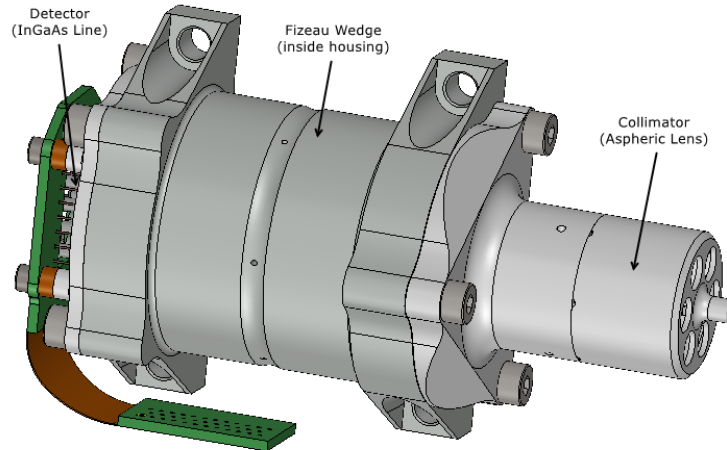


Figure 4. The FRUF wavemeter assembly

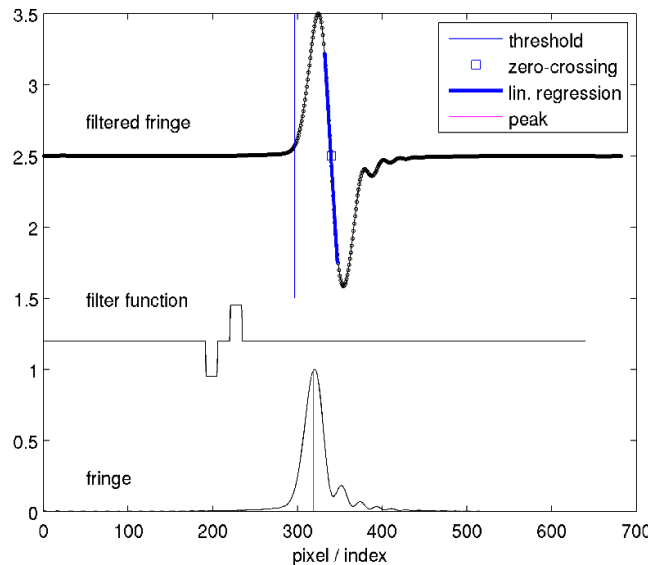


Figure 5. Fringe pattern and signal processing for frequency measurements

For the FRUF assembly a commercial InGaAs line has been procured which is undergoing the qualification process at SpaceTech. For what concerns the optical elements, the qualification approach and effort is the same as it has been described in paragraph 2.4 for the FRUA assembly.

The Fizeau's optical length and therefore the fringe position is quite sensitive to pressure and temperature changes, which needs to be accounted for in the ground testing campaign and the operational concept in space.

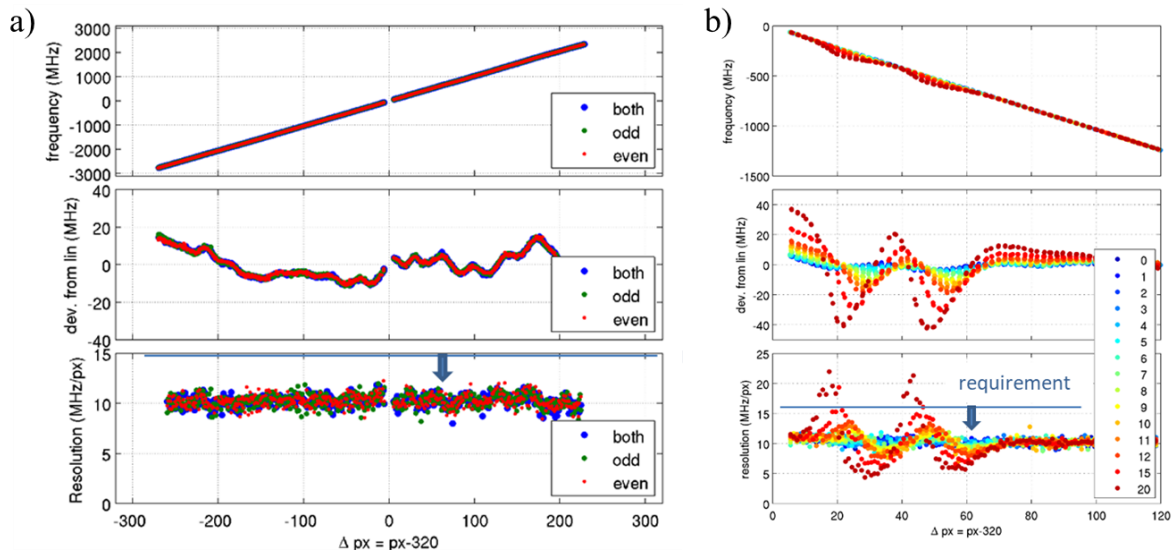


Figure 6. a) Measurement of the wavemeter response and resolution of data recorded by both ROICs in comparison with only data from the odd and only the even pixels. b) Wavemeter linearity and resolution as a function of bad pixels. The region of interest has been zoomed in. (Note that the sign of the frequency axis is reversed, which is only defined by convention.) The first bad pixel is located at the position of  $\Delta px = 50$  and the following bad pixels are introduced at lower  $\Delta px$  positions (50,49,48,...).

## 2.6 The FRU harness and opto-electronics

The optical harness includes tap couplers and optical switches. The tap couplers are all fiber devices, manufactured with a fused biconical taper process. They are bidirectional devices that maintain the polarization of the input. Within the FRU two types of couplers are used: couplers in 2x1 configuration and 2x2 configuration for combination of signals within the FRU and from the ICC. Please refer to Figure 1.

High reliable switches are used for routing the signals of the different laser diodes to the submodules. The switching process relies on change of polarization of an electro-optic material by a short pulse of roughly 0.3 ms. Switching is achieved within the first ten microseconds. After switching, no electric power is necessary to maintain the current status. The device is fiber coupled and polarization maintaining. Electro-optic components within the FRU are connected by optical fiber. Therefore, tens of meters of optical fiber are integrated and contribute to the optical harness. All fibers are coated with UV acrylate and, for some components, an additional buffer of thermoplastic elastomer is needed for manufacturing. Except for a short piece of single mode (SM) fiber in front of the FIA, solely polarization maintaining fibers are used. Thus, the alignment and polarization of the optical path in the FRU is almost unaffected by temperature changes and offers great flexibility in fiber routing. Different components are connected by fiber optic splicing, external by Mini-AVIM fiber connectors. A splice qualification process ensures that the optical connections meet the requirements imposed by the space environment. This includes test of depressurization, temperature, optical performance, routing and fixation of the fibers. Long term reliability of the splices are verified by the process sustaining tensions in the 20 N regime and a rigorous screening of the systems splices including a 10 N proof-test.

The optical switches haven been procured as commercial high reliability parts and undergo a screening and qualification programme at SpaceTech.

## 2.7 The FRU electronics

The FRU provides all typical electrical functions and interfaces required for an optical instrument as MERLIN. The electronic design is accommodated on four modules: the power-, OSC-Seed-, OPO-Seed- and calibration module. A flex-rigid backplane connects all modules together. The power module generates the required supply voltages within the FRU from the primary power bus. The OPO-Seed module electronics can be considered as the master board of the FRU comprising the FPGA as the central element. On this module are also the 1645nm laser diodes and their control and drive electronics. The OSC-Seed module electronics include the 1064 nm laser diodes with their control and drive electronics. The calibration module provides the electrical design and interfaces to control the wavemeter and the measurement of the CH<sub>4</sub> absorption curve by the photo diodes.

### Power electronics

The main primary power bus of the MERLIN satellite is an unregulated direct current (DC) voltage bus with battery connected directly to the bus. The primary voltage range is between 27V and 37V. Two hybrid DC/DC converters and a

Point of Load (POL) converter transform the primary power and provide into all required FRU internal supply voltages (+/-9 V, 5.8 V, 3.3 V and -2.6 V). The converter provides a galvanic isolation to be compliant to the EMC requirements (e.g. distributed single point grounding philosophy). An opto-coupler provides an ON/OFF interface for a low power command signal of 5V to enable the DC/DC converter. In the FRU box, a star point grounding concept is realised. The common or central star ground point is chosen within the power module and individual ground lines are distributed to the modules to avoid ground loops. Because the laser diodes are temperature controlled, the power consumption of the FRU depends on the actual ambient temperature. The maximum power consumption at full performance is approximately 23 W. The fundamental conversion frequency of the DC/DC converter is around 300 kHz, generating integral multiple frequencies on the secondary supply voltages. To reduce the converter noise, low pass PI-filters with a cut off frequency of around 5 kHz are implemented on all secondary supply voltages.

### **OPO-Seed module electronics**

The OPO-seed module electronics comprise two printed circuit boards (PCB) as a piggyback solution. The main board establishes the control circuits and electrical devices, whereas the second board mounted on the main board only includes the 1645 nm laser diodes. The central device on the main board is the FPGA (RT3PE3000 from Microsemi). Two linear voltage regulators generate the 1.5 V core and 2.5 V interface voltage of the FPGA, whereas the power board provides the 3.3 V interface voltage directly via the backplane. Due to the robust single event upset (SEU) behaviour of the FPGA, no latch up protection circuitry is required. The FPGA is running with 40 MHz clock driven by an oscillator.

In total, four individually-controlled laser diode drivers are realised on the board. The laser diode drivers consist of a very high precision DC constant current sink and a very high precision linear driven thermo-electric cooler (TEC) controller. The FPGA provides the actual current and temperature set point levels to the digital to analogue converter (DAC) with a Serial Peripheral Interface (SPI) bus. Each DAC has a resolution of 12 Bits.

To achieve the required current resolution for the OPO-Seed laser diodes, the current sink is divided into two current portions. An offset current is always present if the corresponding laser diode is enabled and, additionally, a variable current with a narrower dynamic range is put on top of the offset current.

A current limiter in series to the laser diode protects the laser diode against occurred transients of the current sink operational amplifier and protects the supply voltage against potential short circuits within the laser diode module in the failure case. The current limiter also includes a transistor switch to enable or disable the current sink. The TEC controller is a discrete-implemented PI regulator. The actual laser diode temperature is measured by a NTC-thermistor equipped to each laser diode module. An analogue-digital-converter (ADC) combined with multiplexer devices acquire the actual laser diode current and the TEC temperature as housekeeping (HK) data.

Three optical switch drivers are on the board. The driver electronics comprises four bipolar transistors arranged as H-bridge. A pulse shape signal toggles the optical position of the switch and keeps the state like a latch relay. To re-toggle the optical position, a further pulse with reversed polarity is required. The switches' timing and triggering are controlled by the FPGA.

The communication (TM/TC) interface to the instrument control unit (ICU) is a SpaceWire (SpW) interface. The connector of the SpW interface is on the OPO-Seed module. Standard LVDS transmitter and receiver devices realise the electrical interface.

### **OSC-Seed module electronics**

The OSC-Seed module electronics are realised in the same way as for the OPO-Seed module with a piggyback solution comprising the main board establishing the control electronics and a mounted board including the laser diode modules. Two laser diode drivers in a redundant configuration are implemented. The FPGA selects the active laser diode driver and provides the set values via a SPI bus.

The electrical circuitry of the laser diode drivers comply with the circuitry of the OPO-Seed module with one exception that no offset current is present. This means that the adjustable laser diode current extends over the full-scale resolution of the DAC. An ADC converts the current of the laser diode and TEC temperature to the FPGA, which provides the monitored values in the TM data as HK values.

### **Calibration module electronics**

The calibration module comprises the wavemeter control electronics and the photodiode amplifiers, measuring the pre- and post- laser signals of the CH<sub>4</sub> cell assembly (FRUA). Each photodiode amplifier is realised as a transimpedance amplifier (TIA) to convert the photodiode current into a corresponding voltage. For redundancy reasons, the photodiodes and its amplifier chains are duplicated.

The InGaAs line detector is part of the wavemeter. The control electronics of the line detector is on the calibration board and consists mainly of the Analogue-Front-End device LM98640 from TexasInstruments and digital control signals

provided by the FPGA. The Analogue-Front-End device is a fully integrated high performance 14-Bit signal processing solution for image processing applications. It integrates two ADC channels operating in parallel with an integrated programmable gain amplifier (PGA) for each channel, converting the analogue output signals from the line detector. The device receives a 5 MHz clock signal from the FPGA and speeds up the clock frequency to a 40 MHz data clock by an internal phase locked loop logic. The converted values are serialised and provided to the FPGA via a dedicated serial interface of LVDS type.

A 5 V voltage regulator supplies the line detector. A latch-up protection circuitry protects the line detector against potential single event latch-ups (SEL). In case of a SEU, the FPGA performs a power cycle of the line detector by disabling and enabling the latch-up protection circuitry.

### Laser Diode Driver

With regard to the optical performance, the development of the laser diode driver has to be emphasized. The frequency stability and noise requirements are challenging. The laser diode driver comprises the following features:

- a controllable laser diode (LD) current source
- a temperature error amplifier, proportional and integral (PI) gain controller and a linear TEC current source
- conditioning amplifiers to monitor the laser diode chip temperature and the Laser Diode current
- Internal Reference Voltage Generation
- 2 Digital-to-Analogue Converters to control the TEC current and the LD modulation current

The maximum TEC current of 650 mA allows a linear power output stage which was preferred to a PWM-controlled power amplifier to avoid signal interference. A temperature conditioning circuitry measures the laser diode temperature in a range from -30°C to +80°C with a NTC thermistor installed in the laser diode module. The FPGA delivers the set value of the laser diode temperature. A PI-regulator followed by bipolar-supplied power stage represents the temperature control loop. The integrational portion of the regulator ensures that there is no remaining control deviation. The set value is limited to the optimum operating point of 30°C +/- 10 K. This offers the advantages against the full measurement range that the resolution is improved and it avoids that a failure in commanding the temperatures damages the laser diode.

Table 1. Performance Summary of Laser Diode Driver

Parameter	OSC-Seed LD	OPO-Seed LD
Offset Current	-	130 mA
Variable Current	0 to 160 mA	0 to 6 mA
Resolution (12 Bit)	29.3uA / bit	1.5uA / bit
Modulation Range	-	0 to +/- 3mA
Max. TEC Current	650 mA	
Temp. Set Range	20°C to 40°C	

The laser diode operates with a current from a constant current sink. At the beginning of the project, space qualified high resolution digital-to-analogue converters (DAC) were not available. The choice fell to a 12Bit DAC from Texas Instruments. A further advantage of this device is the SPI interface.

Two in parallel operating current sinks apply the constant current to the laser diode: a fixed-offset current of 130 mA and a variable current in the range of +/-3 mA commanded by the FPGA with a resolution of 1.5  $\mu$ A per step of the DAC.

Commercial laser diode driver designs can use a variety of highly sophisticated devices which have been developed for best performance such as offset, stability and noise properties. For space application such as MERLIN, initially only a small number of available components could be selected which meet the space-specific environmental requirements. Therefore, it is remarkable that the developed laser diode driver shows a very good noise characteristic comparable with off the shelf designs and as a reference from literature<sup>3</sup> what is needed to have sufficient performance, see Figure 7.

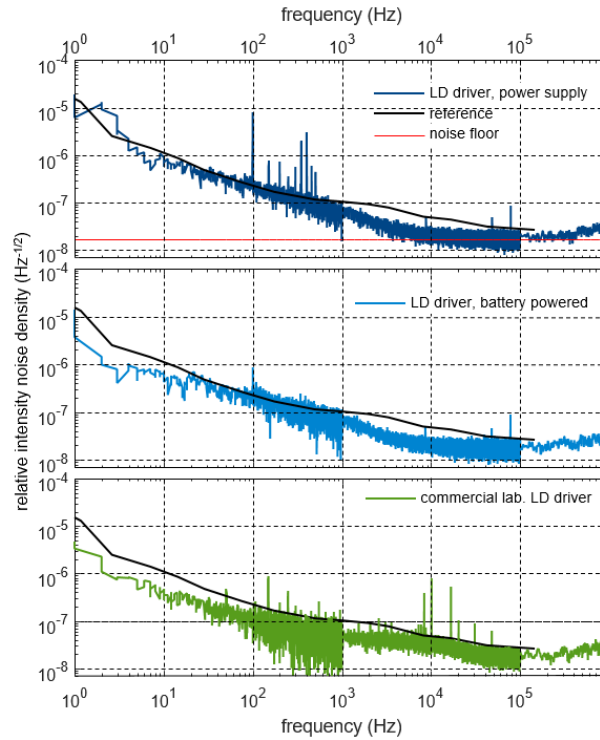


Figure 7. Comparison of noise performance in terms of relative intensity noise of the laser diode driver developed for the MERLIN FRU with a commercial laboratory laser diode driver. The lasers used for characterization are DFB laser diodes with a line width of 1 MHz. The shown reference is from [3].

## 2.8 The FPGA design

A re-programmable FPGA (RT3PE3000L) is used as the central control element of the FRU. It is connected to 10 DACs (12-bit), 4 ADCs (12-bit), 2 MUXes (8-bit), a SpaceWire RMAP port, 18 digital output and 3 input lines and implements four control loops for  $\lambda_{ref}$ ,  $\lambda_{on}$ ,  $\lambda_{off}$ , and the OPO cavity.

The functionality of the FPGA has been broken down into the following main modules (refer to Table 2. ):

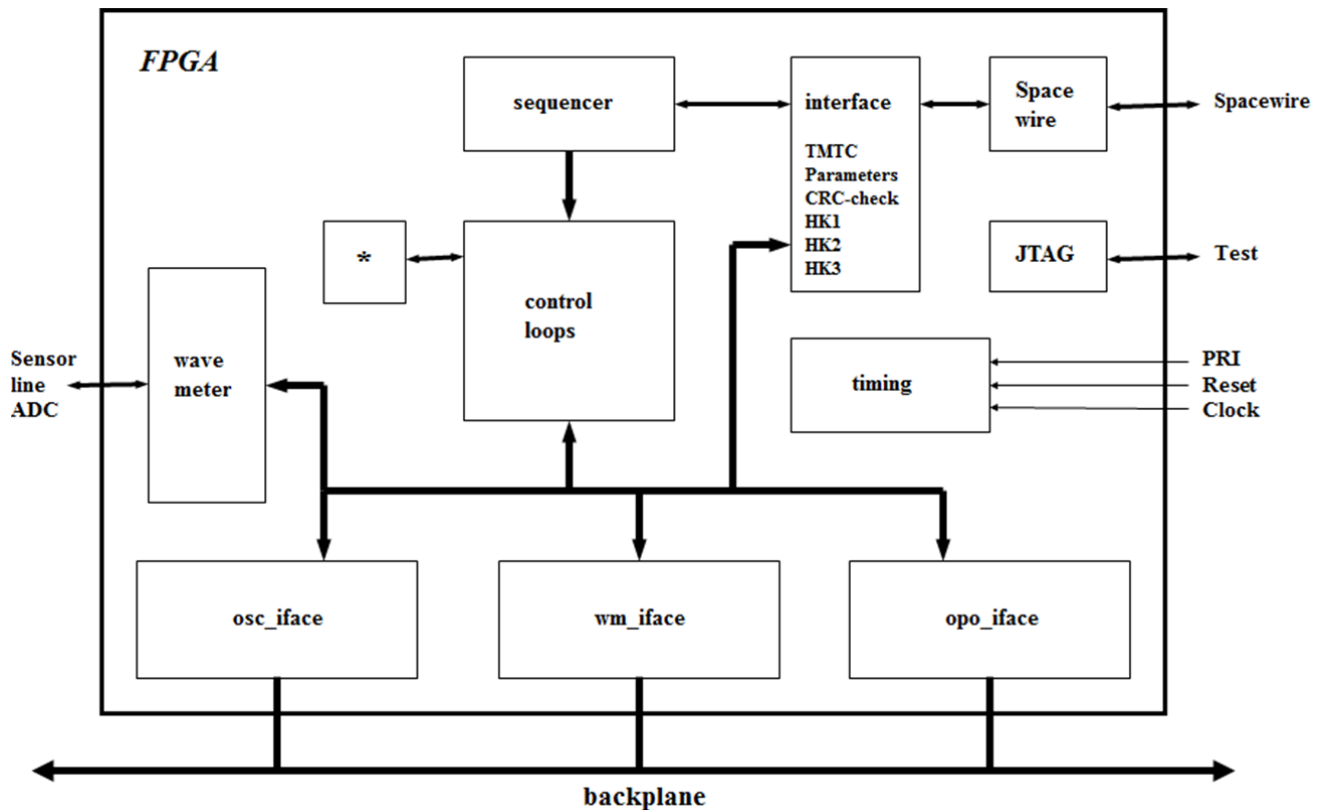
Table 2. Functional modules of the FPGA

Module name	Description
timing	Time services and pulse repetition interval (PRI) processing
SpaceWire	SpW - Spacewire interface to the ICU
interface	ICU communication memory (TM/TC Register, housekeeping data and parameter memory)
opo_iface	OPO-seed laser diode interface
wm_iface	Wavemeter and absolute frequency reference (gas cell assembly) control interface
osc_iface	OSC-seed laser diode interface
wavemeter	Sensor line interface and fringe detector
*	Central multiplier resource
control loops	Four control loops for $\lambda_{ref}$ , $\lambda_{on}$ , $\lambda_{off}$ , and the OPO cavity
sequencer	TM/TC processing and FRU mode control. Diagnostic and Atmospheric Calibration mode supervision.
test	JTAG interface for FPGA configuration, three FPGA outputs as status monitoring signals.

## ICU Interface

Three memory-mapped TM/TC registers and four dedicated memory areas are set aside for communication with the ICU via SpaceWire RMAP:

- Error detection and correction (EDAC) and cyclic redundancy check (CRC) safeguarded memory that serves as storage for the FRU's operational parameters.
- General HK1 housekeeping data, mostly temperatures, which are independent of the control loops.
- Every PRI pulse triggers the computation of housekeeping data representing internal states of the control loops. Upon arrival of the next PRI pulse, the newly computed data is copied into the HK2 memory area that can be read by the ICU during the next PRI cycle.
- HK3 housekeeping data allows the ICU to read the samples of each of the wavemeters' five fringes ( $\lambda_{ref}$ ,  $\lambda_{on}(seed)$ ,  $\lambda_{off}(seed)$ ,  $\lambda_{on}(Tx)$ ,  $\lambda_{off}(Tx)$ ) that are produced during a PRI cycle in operational mode.



• Figure 8. The layout of the FPGA functional modules and the outer interfaces to the peripheral devices and the ICU.

### The FRU Operating Modes

In *CONFIG* mode, a set of 190 operational parameters (16-bit) must be transferred via SpaceWire into the EDAC and CRC safeguarded memory inside the FPGA, because the FRU itself does not have any non-volatile storage.

In *STANDBY* mode, the thermo-electric-coolers of four laser diodes ( $\lambda_{ref}$ ,  $\lambda_{on}$ ,  $\lambda_{off}$ , and OSC) are switched on, regulated by an analogue control loop.

In *DIAGNOSTIC* mode, each of the four seeder diodes separately and the optical switches are stimulated in such a way that the analysis of the HK data will allow to pinpoint hardware faults.

In *OPERATIONAL* mode, the currents for the laser diodes are switched on and the control loops start to operate. When the control loops have synchronized, OPO cavity control data will be transmitted to the OPO via SpaceWire.

*OSC CALIBRATION* mode is a sub-mode of *OPERATIONAL*. While the control loops continue to operate generating HK data, the 1064 nm OSC laser diode will run through a configurable sequence of TEC temperatures and laser diode currents. Later analysis of the HK data allows to select the optimal operating point for the OSC laser diode.

*ATMOSPHERIC CALIBRATION* mode is a sub-mode of OPERATIONAL.  $\lambda_{on}$  will be swept across the six methane absorption lines, which are used as absolute frequency reference. As a consequence,  $OPO_{on}$  will be swept accordingly, such that the absorption lines in the backscatter signal can be recorded.

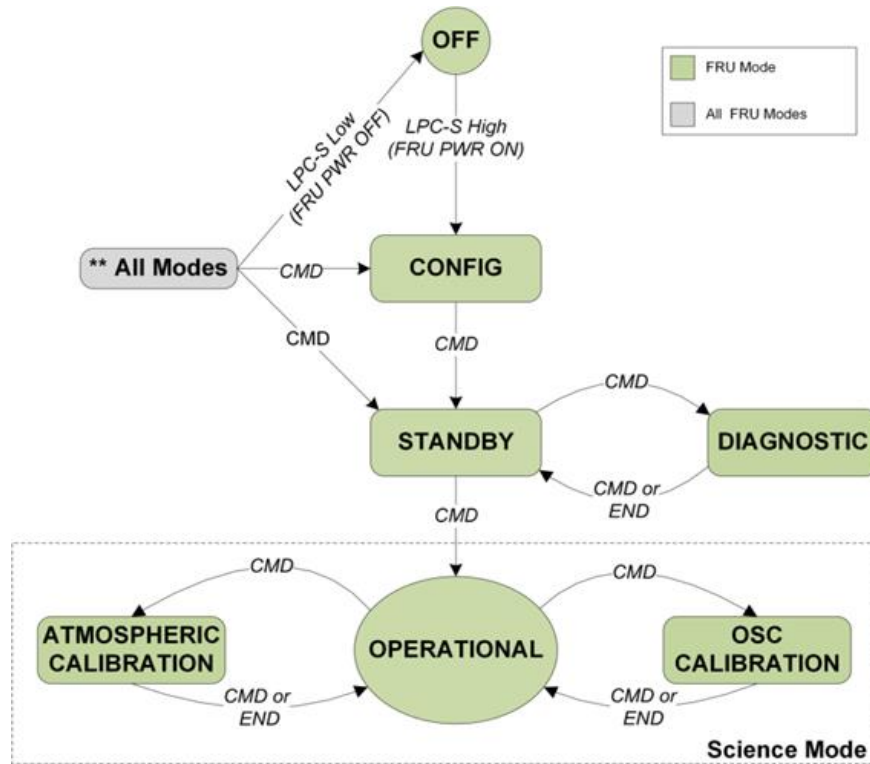


Figure 9. FRU Mode Diagram

### Rapid Prototyping

To speed up FPGA development, a two-phase approach has been used, exploiting the re-programmability of the FPGA:

In the first phase, the sequencer and the control loops have been realized as Forth software running on a so-called micro core ( $\mu$ Core) processor, which is a soft core inside the FPGA.<sup>4</sup> The software could be interactively debugged using a UART Rx/Tx interface on the Test port. The FRU's functional validation suite has been developed on the basis of this processor-assisted design.

In the second phase, the software-based implementation will be trans-coded into VHDL and validated using the previously developed validation suite.

The development speedup was significant: It only takes about 15 seconds to cross-compile, load the object code and start the debugger. Whereas VHDL synthesis, place&route, bit-stream generation and FPGA configuration takes about 30 minutes. Therefore, the FRU's functionality could be developed using a rapid prototyping approach.

The  $\mu$ Core processor is a VHDL hardware embodiment of the virtual machine underlying the Forth programming language, and  $\mu$ Core's "assembler" is the core word set of Forth. It is a Harvard architecture, dual stack, deterministic real-time processor with 300 nsec maximum interrupt latency. Therefore, even in the  $\mu$ Core implementation, the jitter of the most time critical operations (OPO-on and OPO-off frequency measurement) is below 2  $\mu$ s.

### Radiation mitigation

The external Reset and the PRI pulse is fed into the FPGA three times on three different I/O-banks with internal voting, because each I/O-bank is activated/deactivated by a latch, which is potentially susceptible to SEUs.

The FPGA's output pins are tri-stated by the asynchronous Reset signal and safe states are established externally using pull-up/pull-down resistors.

The logic inside the FPGA solely uses a synchronized reset in order to reduce the probability for single event transient-induced resets.

All Flip-Flops inside the design, which hold state information, will use triple modular redundancy.

The parameter memory will use EDAC for single error correction with scrubbing and a CRC, which is continually checked. When the CRC is not valid, the `crc_err`-bit will be set in the status register.

The internal state variables, which need to be valid for more than one PRI cycle, will be stored in EDAC-safeguarded memory with scrubbing.

## 2.9 The mechanical housing and structural design

The mechanical housing consists of the underlying baseplate and four modules perpendicularly oriented to the baseplate. The mechanical design is driven by the functional requirements of the FRU. There are four basic modules: the Calibration module, the OPO-seed module, the OSC-seed module and the Power module. The modules are interconnected to each other by six M5 bolts. This pre-assembly is then mounted onto the baseplate. Due to the dynamic behaviour of the FRU, the components close to the baseplate are the least-stressed components. The modules are thin-walled aluminium housings with stiffening features. This ensures local stiffness. The PCB boards are bolted to the modules, the bolts are placed in a regular pattern on the stiffening ribs. The mechanical environment during launch is very demanding. The sine test loads are specified up to 150 Hz with up to 27 g. The random and shock loads are also very high for a large component (mass > 5 kg) like the FRU. The random loads are specified with 16.9 grms and 12 grms for out-of plane and in-plane respectively. The shock loads are specified with up to 1000 g at 1000 Hz. The structural design aims for minimizing the vibration loads for the optical components. The metallic structures are sufficiently strong; the design is driven by stiffness and minimum milling thicknesses. Still, the final stiffness has to be traded off against the high shock loads. A more rigid structure leads to lower shock dephasing and routes more shock to the critical large optical components.

The analysis of the structure is conducted with Nastran and all environmental tests are supported by these analyses and conducted in-house.

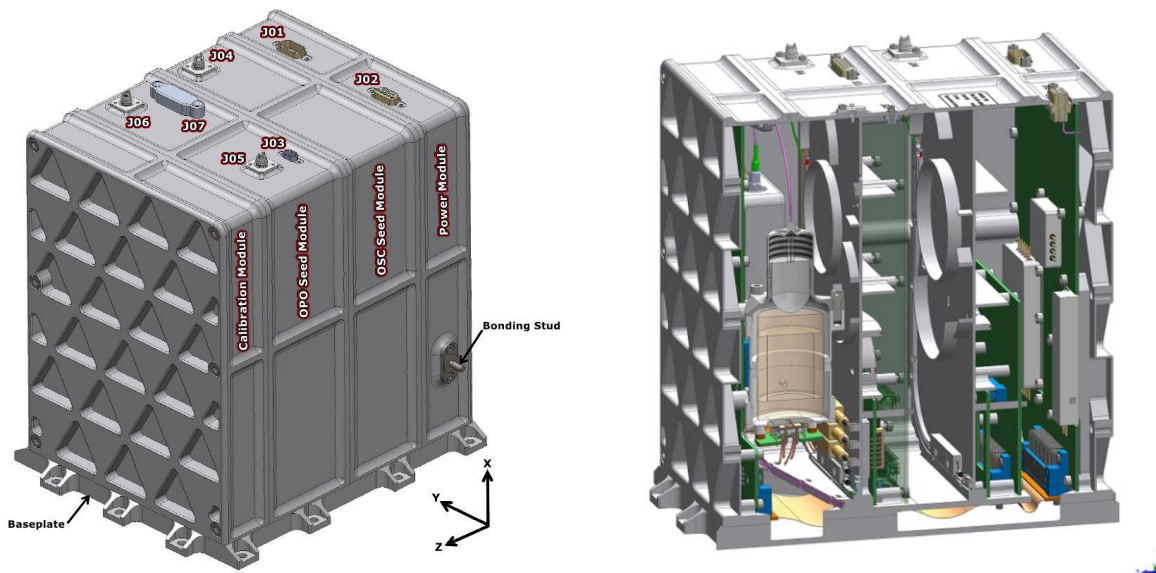


Figure 10. The FRU Configuration. Overall configuration (left) and cut-away view (right)

## 2.10 The thermal design

The thermal design of the FRU is a classical passive system. The FRU dissipates approximately 23 W in nominal science operation mode. It utilizes the main thermal contact to the baseplate. The box housing parts are black anodized for increased heat distribution inside the box. The black surfaces outside radiate directly to the spacecraft radiators adjacent to the FRU –Z direction. The thermal design is driven by the laser diodes. The laser diode temperatures are kept constant at temperatures between 27°C and 33°C (depending on the type and function of the diode) with thermo-electric coolers (TEC). These TEC units dissipate waste heat depending on the temperature difference between interface and diode they have to bridge. In order to avoid a thermal runaway, the box temperature upper limit is the critical driver for the thermal design. The design of the box is therefore equipped with high cross-section aluminium bars between the diode interfaces and the bottom plate. The bottom plate is connected with a spacecraft-supplied heat pipe to the spacecraft-supplied radiator. The radiator-facing side of the FRU is the Power module. Most of the dissipated waste heat is at this power module side of the box. The additional heat path via radiation to the radiator is used. The analysis is conducted with ESATAN TMS, the test predictions of the analysis will be verified by TV testing in-house.

The predicted temperatures of the CDR analysis loop confirms that all component temperature limits are respected.

### 2.11 Main performance data

With the engineering model (EM) that is shown in Figure 11, the following main performance numbers could be achieved:

- The systematic error that is expected from the absolute frequency reference could be confirmed to be in the range of  $\pm 4$  MHz.
- The random error of the wavemeter measurement was found to be  $\pm 2$  MHz.
- In contrast, the non-linearity error of the wavemeter was found to be at the limit or even larger w.r.t the required performance and further engineering has been conducted to restore the margin with the next model.

The EM wavemeter incorporates the monolithic fibre collimator design that will be used in the flight model in contrast to the commercial triplet collimator that was used for the bread board model. During the tests of the EM wavemeter it turned out that the used aspheric lens introduces a non-linearity that is three times larger than what had been found for the bread board wavemeter. Further analysis revealed that the manufacturing process of the aspheric lens leads to periodic distortions in the radial direction, which act like a phase grating and modulates the intensity profile of the collimated beam in the far field. To reduce this major source of non-linearity to an uncritical level, a different production process will be used for the next models.

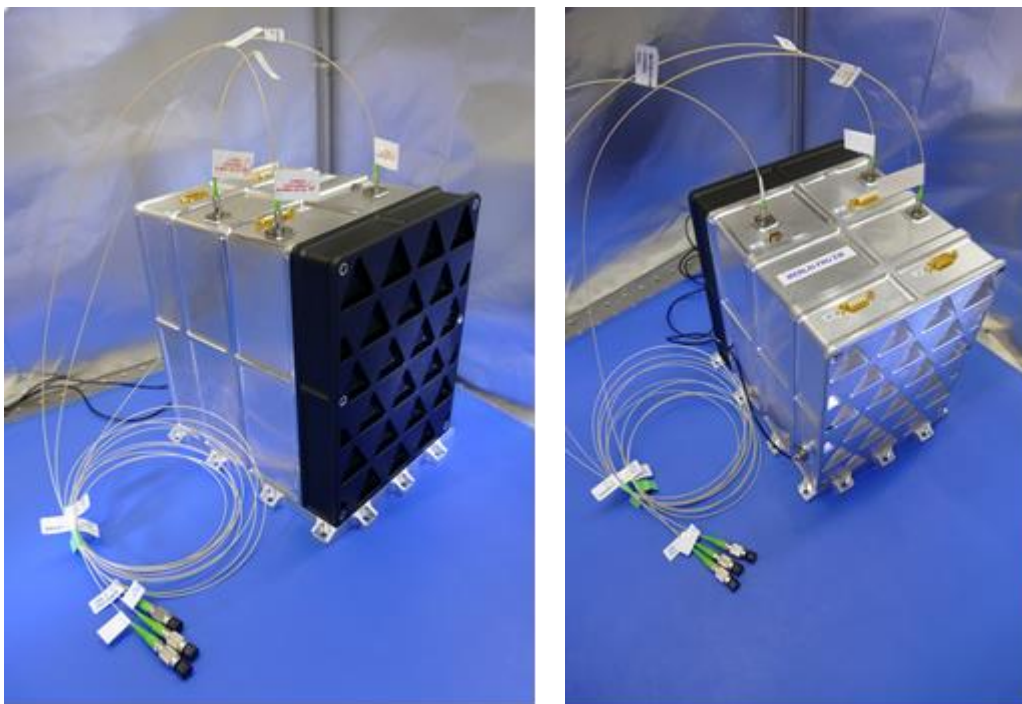


Figure 11. The engineering model of the FRU. Only one out of the four modules has been black anodized like it will be the case for all parts in the later flight design. Three optical patch cords are attached for interfacing the test equipment and finally the laser and ICC of the engineering model of the MERLIN instrument.

## 3. CONCLUSION AND FUTURE PROSPECTS

In this paper, we presented the design of the absolute frequency reference unit for the remote sensing LIDAR Mission MERLIN. The absolute frequency is determined by a laser diode that is frequency-locked to the on-board methane gas cell. With a wavemeter, this reference frequency is transferred with an adjustable frequency offset to two other frequency-locked diode lasers with linewidth, stability and setting accuracies in the low MHz range. They are used to seed the online and offline laser pulses generated in the OPO, which are transmitted to the earth.

Every single pulse pair is again measured on the wavemeter for spectroscopic reasons. Therefore, every single pulse of the nominally 40 per second generated pulses is known with 10 MHz accuracy and provided in the HK data. These can be used for data analysis on ground to improve the overall sensitivity of the methane detection.

Most effort was needed to prove the electro-optic components being qualified for the demanding space and launch environment. In addition, the thermal engineering was crucial in order to have sufficiently stable conditions at the laser diode chips despite the required temperature range from 0°C to 40°C. Vibrational and shock loads are at a critically high level for the free-space optical elements and a trade-off between stiffness and shock dephasing had to be done.

The engineering model validated the required performance except for the non-linearity of the wavemeter where further engineering has been conducted to restore the performance that could already be achieved with the bread board FRU.

During phase C/D of the FRU development, it has been determined that the wavemeter is the performance-limiting, critical element and additional efforts were required to recover the required performance. Regarding future missions that need higher frequency accuracies (e.g. detection of CO<sub>2</sub>), an alternative to the wavemeter will be needed. SpaceTech is going to develop such alternative methods in other projects.

## REFERENCES

<sup>1</sup> Ehret, G., Bousquet, P., Pierangelo, C., Alpers, M., et al., “MERLIN: A French-German Space Lidar Mission Dedicated to Atmospheric Methane”, *Remote Sens.* 2017, 9(10), 1052.

<sup>2</sup> Heinecke, D., Liebherr, T., Diekmann, C., et al., , “The absolute frequency reference unit for the methane-sensing lidar mission MERLIN”, *Proc. SPIE 10562, International Conference on Space Optics — ICSO 2016.*

<sup>3</sup> Numata et al., “Performance of planar-waveguide external cavity laser for precision measurements”, *Optics Express* 18(22) pp.22781 (2010).

<sup>4</sup> Knecht, M., Meier, W., Schleisiek, K., Nicola, C. U., “Software/Hardware Co-design: Crypto MicroCore”, FOKUS REPORT 2014, Institut für mobile und verteilte Systeme, Fachhochschule Nordwestschweiz, pp.39, <<https://www.fhnw.ch/de/die-fhnw/hochschulen/ht/institute/institut-fuer-mobile-und-verteilte-systeme/publikationen/media/fokus-report-2014.pdf>>.